Available online at www.sciencedirect.com
SCIENCE DIRECT
Polymer 46 (2005) 109–119
polymer
www.elsevier.com/locate/polymer

Structure and swelling behaviour of epoxy networks based on α,ω-diamino terminated poly(oxypropylene)-*block*-poly(oxyethylene)-*block*-poly(oxypropylene)

Ivan Krakovský[a,*], Jan Hanuš[a], Josef Pleštil[b], Josef Baldrian[b], Manuel Salmerón Sánchez[c]

[a]*Department of Macromolecular Physics, Faculty of Mathematics and Physics, Charles University, V Holešovičkách 2, 180 00 Prague 8, Czech Republic*
[b]*Institute of Macromolecular Chemistry, Academy of Sciences of the Czech Republic, Heyrovský Sq. 2, 162 06 Prague 6, Czech Republic*
[c]*Centro de Biomateriales, Universidad Politécnica de Valencia, Camino de Vera s/n, Valencia, Spain*

Received 22 March 2004; received in revised form 7 October 2004; accepted 20 October 2004
Available online 23 November 2004

Abstract

Structure and swelling behaviour of hydrophilic epoxy networks prepared from α,ω-diamino terminated poly(oxypropylene)-*block*-poly(oxyethylene)-*block*-poly(oxypropylene) and diglycidyl ether of brominated Bisphenol A in dependence on the initial molar ratio of reactive amino and epoxy groups has been investigated by small- and wide-angle X-ray scattering (SAXS and WAXS), differential scanning calorimetry (DSC) and dynamic mechanic analysis (DMA). Anomalous swelling behaviour of the networks in water has been found. The anomaly is attributed to the changing microphase separation in the networks controlled by their composition and crosslinking density, and inhomogeneous swelling on nanometer space scale.

Keywords: Epoxy network; Microphase separation; Swelling

1. Introduction

Epoxy resins are a class of industrially important polymer materials with a wide versatility of structure, low shrinkage during curing, good alkali resistance, excellent mechanical, thermal and dielectric properties. Therefore, they have found many applications as adhesives, coatings or castings [1]. Due to convenient mechanical properties, epoxy resins are also used as matrix material in fibre-reinforced composites [2,3].

Epoxy resins are usually prepared by the reaction of diamino-functionalized prepolymer with a diepoxide, e.g. α,ω-diamino terminated polyoxypropylene (POP) with diglycidyl ether of Bisphenol A (DGEBA), during which the initially liquid reaction mixture passes through a gel-point and converts to a solid three-dimensional polymer network. By using α,ω-diamino terminated polyoxyethylene (POE) hydrophilic networks can be prepared; however, high reactivity of amino groups in this case can be a disadvantage in some applications. α,ω-diamino terminated poly(oxypropylene)-*block*-poly(oxyethylene)-*block*-poly(oxypropylene)s (Jeffamine® ED series) are less reactive and epoxy networks prepared from them can have attractive properties in biomedical applications.

Meloun et al. [4] investigated by SAXS and photoelastic measurements various bimodal epoxy networks prepared by curing mixtures of diamines and triamines of POP various molecular weights with DGEBA. They have found clustering of POP chains in the networks.

Beck Tan et al. [5] used small-angle X-ray scattering (SAXS) and differential scanning calorimetry (DSC) for investigation of bimodal epoxy graft copolymers and bimodal epoxy networks prepared by curing mixtures of α,ω-diamino terminated POP of various molecular weight with diglycidyl ether of brominated Bisphenol A (Br-DGEBA). Brominated diepoxide was used to increase scattering contrast for X-rays. They have found that the

* Corresponding author. Tel.: +420 2 2191 2369; fax: +420 2 2191 2350.
E-mail address: ivank@kmf.troja.mff.cuni.cz (I. Krakovský).

0032-3861/$ - see front matter © 2004 Elsevier Ltd. All rights reserved.
doi:10.1016/j.polymer.2004.10.073

results obtained with the bimodal epoxy graft copolymers can be interpreted using random-phase approximation without a need to assume microphase separation. However, they have not found a satisfactory explanation of the results obtained for the bimodal epoxy networks.

The objective of this work was to study the structure and properties of hydrophilic epoxy networks prepared from Jeffamine ED2003 and Br-DGEBA (see Scheme 1) in dependence on the stoichiometric ratio of reactive amino and epoxy groups. The networks were prepared in excess of amino groups. The structure and properties of the networks swollen in water and toluene have been also investigated.

2. Experimental

2.1. Materials and sample preparation

The networks were prepared from Jeffamine® ED2003 (Huntsman) and diglycidyl ether of brominated Bisphenol A (Br-DGEBA, Fluka). Before using, ED2003 was dried at 60 °C for 48 h in a vacuum oven. Concentrations of reactive groups (amino and epoxy) in ED2003 and Br-DGEBA determined by titration were $c_{NH2}=0.95\times10^{-3}$ mol g^{-1} and $c_E=2.28\times10^{-3}$ mol g^{-1}, respectively. ED2003 contains about 60 wt% of POE. A series of networks was prepared at various values of molar ratio of reactants, r, $r=2[NH_2]_0/[E]_0=1.00$, 1.12, 1.25, 1.50, 2.00 (samples EP1, EP2, EP3, EP4, EP5, see Table 1), where $[NH_2]_0$, and $[E]_0$ are initial molar concentrations of amino and epoxy groups, respectively. Both components were first mixed at 100 °C for about 15 min and then poured into Teflon molds. Curing reaction proceeded at 120 °C for 48 h in nitrogen atmosphere.

Because the networks prepared are hydrophilic, they were stored in a desiccator and dried at 70 °C in vacuum oven before further investigation. All networks were transparent.

Table 1
Initial molar ratio of reactants, r, experimental and calculated densities of the dry networks at 20 °C, d_{net}

Sample	r	d_{net}(exp) g cm^{-3}	d_{net}(calc) g cm^{-3}
EP1	1.00	1.361	1.346
EP2	1.12	1.330	1.325
EP3	1.25	1.318	1.305
EP4	1.50	1.281	1.274
EP5	2.00	1.227	1.232

2.2. Measurements

2.2.1. Density

Density of dry networks before and after extraction was determined by double weighing of samples immersed in an inert liquid. Density of Br-DGEBA and ED2003 at 20 °C were determined by pycnometric method.

2.2.2. Extraction and swelling

The weight fractions of sol were determined from the weight decrease after a triple extraction of the samples in toluene at room temperature. After the extraction the samples were dried, first in air, later in vacuum oven at 70 °C for 48 h and the weight in the dry state was measured. Dry samples were swollen in distilled water or toluene at 20 °C and periodically removed, surface-dried and quickly weighed in order to determine the weight increase. Equilibrium swelling ratio Q, was calculated as the ratio of the weight of swollen sample, m, and that of dry sample after extraction, m_0.

2.2.3. Dynamic mechanical analysis

For DMA measurements, rectangular samples of about 15 mm in length and 4 mm in width were cut from the sheets of networks of the thickness about 1 mm. Experiments were carried out using DMA 7e a dynamic mechanical analyser (Perkin–Elmer) in extension mode. Moduli at 20 °C were measured in a creep experiment. Five experiments with

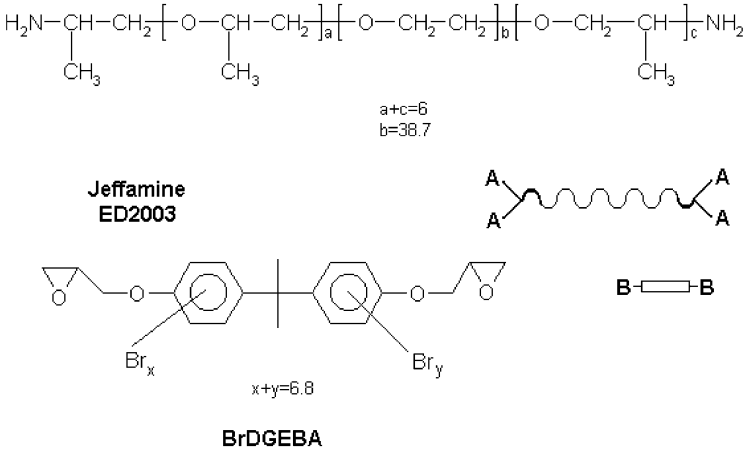

Scheme 1. Schematic representation of diamine and diepoxide.

increasing load (load rate 50 mN/min) were performed and values of Young modulus were calculated from the average of initial slopes of the stress–strain characteristics. Temperature dependence of the complex Young modulus, $E = E' + iE''$, was determined in an oscillating force experiment at frequency $f = 10$ Hz during heating at 5 °C/min.

2.2.4. Wide-angle X-ray scattering

WAXS experiments were carried out on a HZG4A diffractometer (Freiberger Präzisionsmechanik, Germany) using Ni-filtered Cu K_α radiation.

2.2.5. Small-angle X-ray scattering

Swollen samples for SAXS were prepared by multiple extraction of rectangular pieces of dry networks, then dried and immersed in sufficient amount of distilled water. SAXS patterns were measured by Kratky camera with slit collimation using Cu K_α radiation with wavelength $\lambda = 1.542$ Å. Intensities were transformed to smeared differential scattering cross-section (absolute scale), $d\tilde{\Sigma}/d\Omega(q)$, with a Lupolen sample as a secondary standard [6], using the relationship

$$\frac{d\tilde{\Sigma}}{d\Omega}(q) = \frac{a\tilde{I}(q)}{\tilde{I}_L K_L T h} \tag{1}$$

where $\tilde{I}(q)$ is the measured intensity, $q = (4\pi/\lambda)\sin\theta$ is the magnitude of the scattering vector, 2θ is the scattering angle, a is the sample-detector distance. T and h are transmission and thickness of the sample, respectively, K_L is the calibration constant and $\tilde{I}_L$ is the intensity of radiation scattered by the standard at $q = (2\pi/150)$ Å^{-1}.

The mean-square scattering density fluctuation, $\langle(\Delta\rho)^2\rangle$ was calculated from Ref.[7]

$$\langle(\Delta\rho)^2\rangle = \frac{K}{4\pi^2}\int_0^\infty q\frac{d\tilde{\Sigma}_c}{d\Omega}(q)dq \tag{2}$$

where $d\tilde{\Sigma}_c/d\Omega(q)$ is the scattering cross-section corrected for the background scattering using the Vonk empirical formula [8]

$$\frac{d\tilde{\Sigma}_c}{d\Omega} = \frac{d\tilde{\Sigma}}{d\Omega} - (A_1 + A_2 q^m) \tag{3}$$

Here, A_1 and A_2 are empirical constants; best fits were obtained using $m = 1$.

The characteristic scale of inhomogeneity, D_B, was calculated from the position of scattering peak, q_{max}, on the desmeared SAXS profiles using the Bragg equation:

$$D_B = \frac{2\pi}{q_{max}} \tag{4}$$

Further, we calculated the specific inner surface using equation [9]:

$$\frac{S}{V} = \pi v_1 v_2 \frac{\lim_{q\to\infty} q^3 \frac{d\tilde{\Sigma}_c}{d\Omega}(q)}{\int_0^\infty q\frac{d\tilde{\Sigma}_c}{d\Omega}(q)dq} \tag{5}$$

2.2.6. Differential scanning calorimetry

Differential scanning calorimetry was performed using a Pyris 1 DSC (Perkin–Elmer). Samples with a typical weight of ca. 10 mg were examined both in heating and cooling runs with heating/cooling rate ± 20 °C/min. The apparatus was calibrated using distilled water and mercury as standards. The purge gas was helium. Glass transition temperatures were determined using the half Δc_p on the calorigrams from the second heating runs. Crystallisation and melting temperatures were determined from the onsets of heat flow in heating (cooling) runs.

3. Results and discussion

The amine-epoxy curing reaction is described by the well-known kinetic scheme in which the reaction of a primary amine function with an epoxy group leads to a secondary amine which can further react with another epoxy group (Scheme 2). Hydroxy groups formed can also react with epoxy groups; however, at the reaction temperature used, their reactivity is much lower than that of amine groups of both kinds. Moreover, in excess of amino groups the participation of hydroxy groups in the reactions can be neglected.

Since primary amino groups are usually more reactive [10,11], long diepoxy-diamine chains are formed at the beginning of the reaction and branched and crosslinked later on. Therefore, except for the stoichiometric reaction mixture, the structure of resulting networks depends on the relative reactivities of primary and secondary amino groups.

Topology of the stoichiometric and non-stoichiometric network prepared from ED2003 copolymer is illustrated schematically in Fig. 1. Diepoxide molecules themselves form long chains to which diamine chains are grafted by terminals. In the stoichiometric network, a single diepoxide chain of macroscopic length entangled into the POE and POP matrix would be formed under hypothetical perfect reaction conditions. The experimentally determined values of the density of dry networks (see Table 1) are close to the values calculated using densities of ED2003 and Br-DGEBA at 20 °C ($d_{ED2003} = 1.07$ g cm^{-3} and $d_{Br\text{-}DGEBA} = 1.96$ g cm^{-3}, respectively) and assuming additivity of their volumes.

Fig. 2 shows the dependence of the weight fraction of sol on the stoichiometric ratio, r. Experimental data are vertically shifted relative to the data calculated using the theory of branching processes (TBP, see Appendix). This discrepancy is small and can be explained by the presence of a small amount of a nonreactive impurity in diamine or/and diepoxide. Alternatively, the discrepancy can be also attributed to increased formation of cyclic products as it is claimed by some authors in studies of similar systems [12,13]. The discrepancy could be made smaller by including

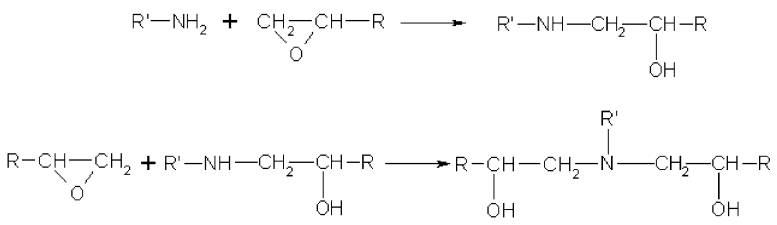

Scheme 2. Reactions involved in epoxy network formation.

these effects into TBP formulas [12], however, this is not necessary for the purpose of this study.

Fig. 3 presents the temperature dependence of the mechanical storage modulus and tangent of mechanical losses for dry networks during heating from −100 to 50 °C. For networks EP1 – EP4, the distinct glass transition is found. With increasing non-stoichiometry, the glass transition temperature has lower values due to increasing mobility of polymer segments with decreasing crosslinking density and growing amount of sol acting as a softener. In network EP4 ($r=1.50$), from ca. −30 °C, the storage modulus grows again and reaches a maximum at ca −10 °C. Because the networks were cooled down quickly from room temperature to −100 °C before the DMA measurement, this effect can be attributed to the crystallisation of POE blocks during heating starting at low temperature; the POE crystallites formed in this way act as a filler. The network density is insufficient to suppress the POE crystallisation at the heating rate used. At temperatures above 10 °C, the crystallites melt and the storage modulus of the sample returns to a value characteristic of amorphous rubbers. As the POE content in the network EP5 ($r=2.00$) is even higher and crosslinking density lower, the (more intensive) crystallisation starts at lower temperature and overlaps the glass transition region.

In Fig. 4, the dependence of the reduced Young modulus measured at 20 °C on the initial molar ratio of reactive group r is shown. Experimental (non-equilibrium) values decrease monotonically with increasing ratio r; they are close to the dependence predicted using the affine model of rubber elasticity and network parameters calculated using the theory of branching processes (see Appendix). A small difference can be attributed to the non-equilibrium character of the experimental determination and/or network defects mentioned above which are disregarded in the simplest version of TBP used.

Fig. 5 shows the dependence of the equilibrium swelling ratio Q on stoichiometric ratio r. It is interesting that while the swelling in toluene is increasing with stoichiometric ratio, in water it passes through a minimum at $r\approx1.12$. At the temperature of swelling (20 °C), toluene is a good solvent for all components of the network (POE, POP and Br-DGEBA chains, see Fig. 1) and swelling increases with decreasing crosslinking density of the networks. Unlike toluene, water at 20 °C is a good solvent only for POE; however this fact itself cannot explain the anomalous swelling observed as the swelling degree should grow with increasing r due to increasing amount of hydrophilic component and decreasing crosslinking density. The explanation of the anomaly will be given below in the light of SAXS and DSC measurements.

WAXS diffractograms obtained for dry networks at 20 °C exhibit a broad scattering maximum around $2\theta\approx22°$. Consequently, amorphous structure of all networks at this temperature can be concluded.

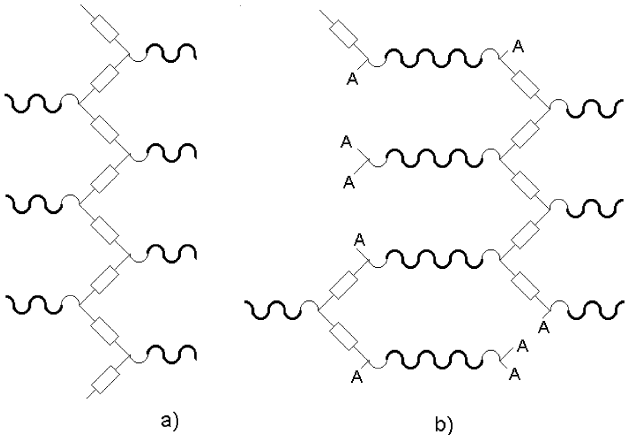

Fig. 1. Schematic representation of the network topology: (a) stoichiometric network, (b) non-stoichiometric network.

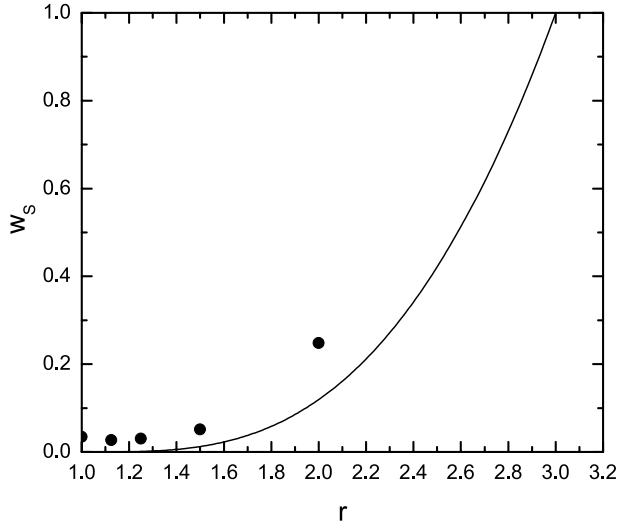

Fig. 2. Experimental and calculated dependence of weight fraction of sol, w_S, on stoichiometric ratio r.

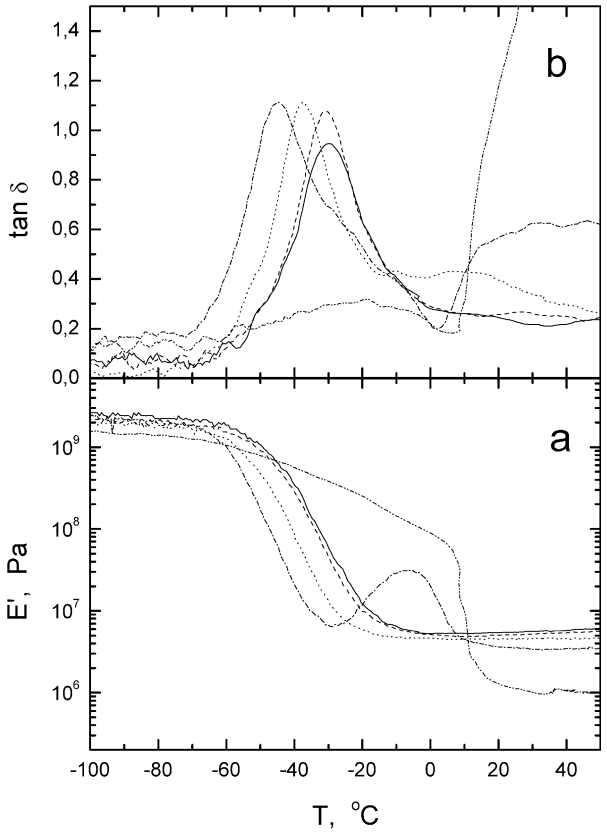

Fig. 3. The temperature dependence of the (a) storage Young modulus E' and (b) tangent of mechanical losses, tan δ (b) for extracted and dried networks measured at $f=10$ Hz. Lines are: (—) EP1, (– – –) EP2, (…) EP3, (-·-·-·-) EP4, (-···-···-···-) EP5.

Fig. 6 shows smeared SAXS curves for dry networks. As the X-ray scattering length densities of POE and PPO are close ($\rho_{POE}=1.00\times10^{11}$ cm^{-2}, $\rho_{POP}=0.95\times10^{11}$ cm^{-2}), the scattering originates almost exclusively from the

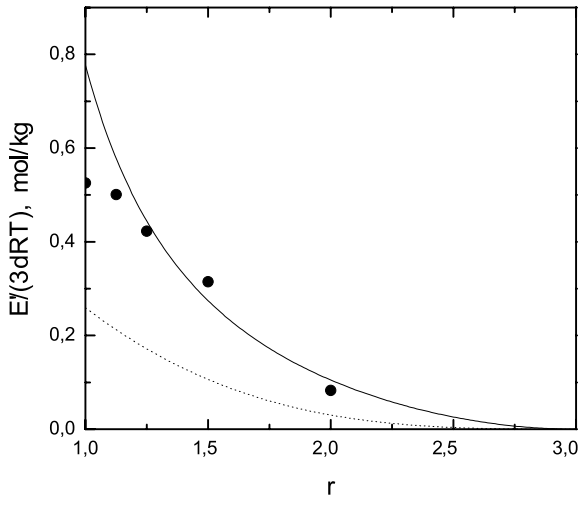

Fig. 4. Comparison of the (non-equilibrium) experimental (●) and (equilibrium) theoretical dependences of the reduced storage Young modulus on stoichiometric ratio r calculated using affine (– – –) and phantom (-·-·-·-) models of rubber elasticity.

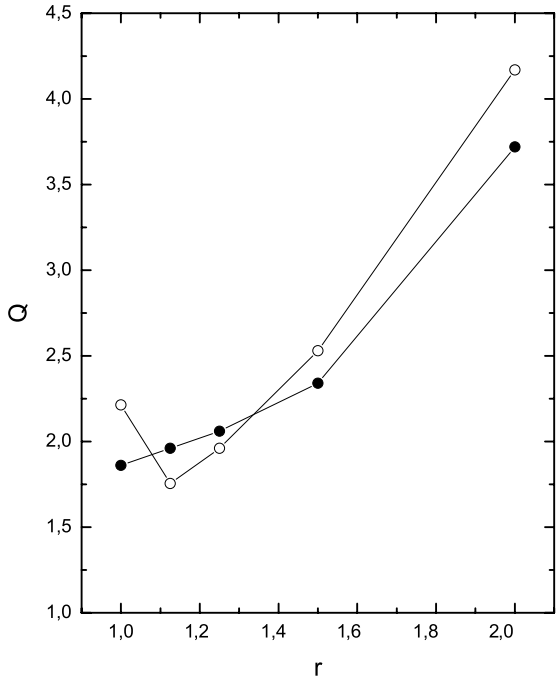

Fig. 5. Equilibrium swelling ratio Q of the networks swollen in toluene (●) and water (○) at 20 °C.

correlation between Br-DGEBA units ($\rho_{Br\text{-}DGEBA}=1.96\times10^{11}$ cm^{-2}). Two scattering maxima are present in all patterns, the broad one at $q\approx0.1$ Å^{-1} can be attributed to the correlation hole effect between the units in different chains, the other at $q\approx0.5$ Å^{-1} to the correlation between the units from in the same chain (see Fig. 1). However, to explain of the order and magnitude of SAXS curves in Fig. 6 (magnitude of scattering intensity decreases in the order: EP2, EP3, EP1, EP4, EP5), this fact is not sufficient and

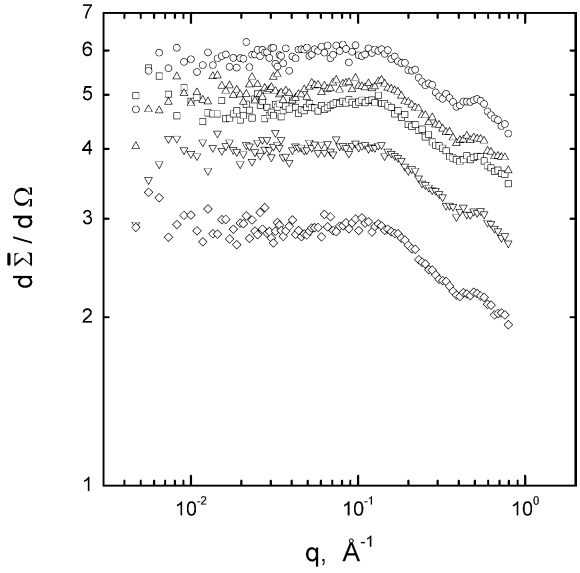

Fig. 6. SAXS patterns of the dry networks (smeared differential cross-section, $d\tilde{\Sigma}/d\Omega(q)$, vs. magnitude of the scattering vector, q. Symbols are: (□) EP1, (○) EP2, (△) EP3, (▽) EP4 and (◇) EP5.

microphase separation has to be also taken into account. Degree of microphase separation in the networks depends on their stoichiometry and can be explained as a result of balance between two opposite factors: the average length of Br-DGEBA chains formed in the reaction and network crosslinking density. In the stoichiometric network, Br-DGEBA chains are the longest and, consequently, tend to the highest degree of the microphase separation. On the other hand, the crosslinking density in this network is the highest and acts oppositely i.e., tends to lower the degree of the microphase separation. An increase in stoichiometric ratio r leads to shorter Br-DGEBA chains; however, the crosslinking density is also smaller and allows higher degree of microphase separation. At higher r values, both the length of Br-DGEBA chains and crosslinking density are too low and a lower degree of the microphase separation can be expected again. (Actually, at higher r values the crosslinking density is low enough to allow crystallisation of POE blocks).

Swelling of the networks in water leads to much stronger X-ray scattering in the region of smallest q (see Fig. 7). The SAXS smeared intensity in the Porod region scales approximately as -3, therefore, a microphase separated structure is expected. To confirm this idea, the mean-square of scattering density, $\langle(\Delta\rho)^2\rangle$, was calculated using

$$\langle(\Delta\rho)^2\rangle = v_1 v_2(\rho_1 - \rho_2)^2 \tag{6}$$

where v_1, ρ_1 and v_2, ρ_2 are volume fractions and scattering length densities of the two different phases.

Two models were analysed. In model A, one phase is assumed to consist of Br-DGEBA chains, the other one of the mixture of POE, POP segments with water. In mode B, one phase consists of Br-DGEBA and POP, the other one of POE and water. The scattering length density of a phase, ρ, was calculated from its density, d, by

$$\rho = \frac{\sum_i Z_i}{\sum_i M_i} N_A b d \tag{7}$$

where Z_i and M_i are atomic numbers and weights of the elements the phase consists of, $b = 2.82 \times 10^{-13}$ cm is the scattering length for a single electron according to Thomson's formula and $N_A = 6.023 \times 10^{23}$ mol^{-1} is the Avogadro constant. Additivity of volumes was assumed in the calculation of phase densities.

Since sol was removed from the swollen networks by extraction, a possible change of the composition of networks has to be taken into account in calculations of the scattering length density of the polymer phase. However, at low contents of sol ($w_S < 0.3$) the difference is small and can be ignored.

It can be seen in Table 2 that except for network EP5 experimental values of $\langle(\Delta\rho)^2\rangle$ lie between the values obtained for models A and B. This means that a part of POP is involved in hydrophobic regions. The values of the specific inner surface and Bragg's distance indicate the nanometer size of the microphase separated structure. These observations agree well with conclusions based on the microphase-separated structure of dry networks. In the dry network EP2, degree of microphase separation is the highest (see Fig. 6) and the fraction of the system swollen with water (POE) is the smallest. Therefore, this network swells less in water. In the rest of networks, degree of microphase separation is smaller and a bigger part of hydrophobic fraction is dragged into swelling.

Fig. 8(a) shows the calorigram obtained during cooling of dry networks and ED2003 at 20 °C min^{-1}. Crystallisation of POE occurs in ED2003 only ($T_c \approx 15$ °C); in all networks it is completely suppressed at this cooling rate. On the other hand, interestingly, during heating (heating rate 20 °C min^{-1}, see Fig. 8(b)), crystallisation and melting of POE occurs in two networks with low crosslinking densities, $r = 1.50$ and 2.00 (EP4 and EP5), crystallisation in EP5 starts ca. -25 °C and melting ends at ca. 30 °C. This agrees approximately with the temperature region in which an increase in storage modulus is observed for EP4 and EP5, although, DSC and DMA measurements were carried out at different heating rates.

With increasing amount of ED2003 and, consequently, decreasing crosslinking density, the glass transition temperature should decrease. Except for the stoichiometric network, the values of the glass transition temperature determined in the second heating runs (see Table 3) confirm the expected trend. The plot of the dependence of reciprocal glass transition temperature on the weight fraction of ED2003 presented in Fig. 9 reveals an anomaly in the expected trend. The values of the reciprocal glass temperature obtained for networks EP2 and EP3 are somewhat lower than the values expected from the composition dependence described by the formula

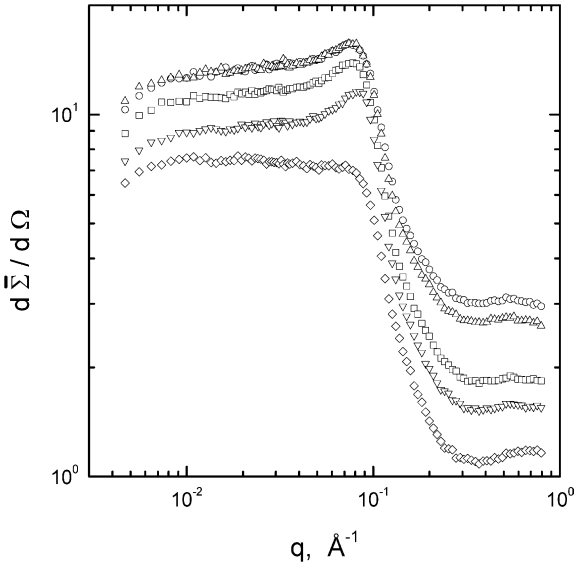

Fig. 7. SAXS patterns of the networks swollen in water. Symbols are: (■) EP1, (○) EP2, (△) EP3, (▽) EP4 and (◇) EP5.

Table 2
SAXS characteristics of swollen epoxy networks

Sample	$\langle(\Delta\rho)^2\rangle$ (model A) ($\times 10^{20}$ cm^{-4})	$\langle(\Delta\rho)^2\rangle$ (model B) ($\times 10^{20}$ cm^{-4})	$\langle(\Delta\rho)^2\rangle$(exp) ($\times 10^{20}$ cm^{-4})	S/V Å^{-1}	D_B Å
EP1	3.93	2.46	2.48	0.044	81
EP2	4.59	2.66	3.04	0.055	85
EP3	3.89	2.19	3.03	0.054	85
EP4	2.69	1.45	2.13	0.045	78
EP5	1.13	0.56	1.50	0.039	–

Specific inner surface, S/V; Bragg distance, D_B; and mean-square scattering density, $\langle(\Delta\rho)^2\rangle$ determined experimentally and calculated assuming two models. Model A: phase 1 = Br-DGEBA, phase 2 = POE + POP + water. Model B: phase 1 = Br-DGEBA + POP, phase 2 = POE + water.

$$\frac{1}{T_g} = \frac{w_{ED2003}}{T_{gED2003}} + \frac{1 - w_{ED2003}}{T_{g,Br-DGEBA}} \quad (8)$$

where w_{ED2003} is weight fraction of ED2003 in the network and $T_{g,ED2003}$ and $T_{g,Br\text{-}DGEBA}$ glass transition temperatures of ED2003 and Br-DGEBA chains, respectively. This anomaly can be explained again by an increased degree of microphase separation and, consequently, a decreased mobility of polymer chains in EP2 and EP3 networks.

Fig. 10 shows the DSC scans for the networks swollen to equilibrium in water. Distinct endothermic peaks attributed to the crystallization of the supercooled water are clearly visible. The crystallization enthalpies are not proportional to the amount of water in the swollen networks (see Table 4).

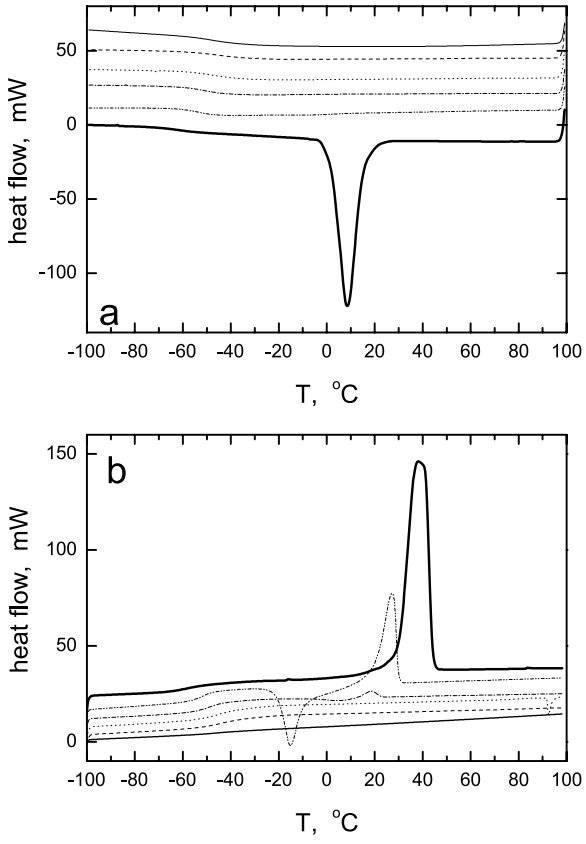

Fig. 8. DSC traces obtained for the dried networks in (a) First cooling at −20 °C min^{-1} and (b) Second heating at 20 °C min^{-1}. Lines are: (—) EP1, (– – –) EP2, (…) EP3 (-·-·-·-) EP4, (-··-··-··-) EP5 and (—) ED2003.

The peak position depends on the content of absorbed water: the lower the content the lower crystallization temperature.

Standard thermodynamics of binary systems predicts that the crystallization (and melting) temperatures of the solvent will experience a cryoscopic depression with respect to the crystallization (and melting) temperatures of the neat component. The crystallization and melting temperatures are functions of composition, which gives rise to the liquidus and crystallization curve in a phase diagram. Since the amount of equilibrium water in the networks varies, the crystallization and melting temperatures of water differ. Besides, in some calorigrams (see Fig. 10(b)) a smaller second peak appears (around −15 °C on cooling and 0 °C on heating), which can be attributed to domains of bulk water in the sample i.e., water that is not homogeneously mixed with polymer chains. However, it is known that the reason for lowering Tm in a system is not only the cryoscopic effect but also the formation of crystals of different dimensions (the Gibbs–Thomsom equation): water that segregates from the swollen polymer does not form a

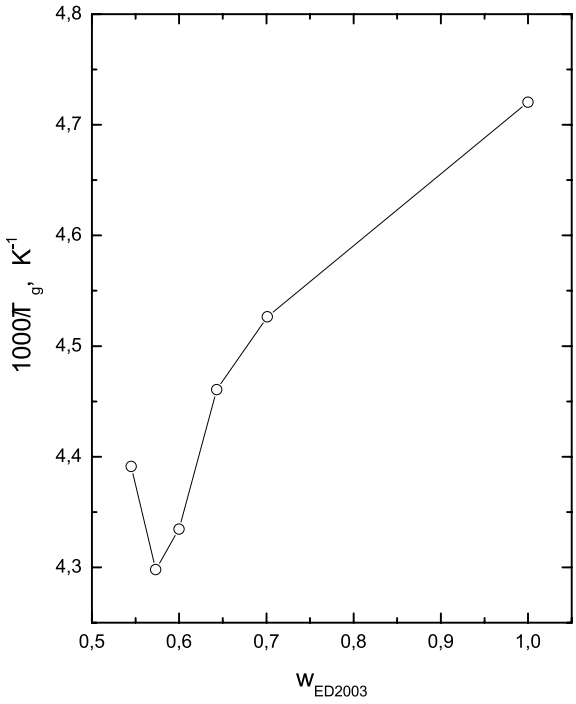

Fig. 9. Plot of reciprocal glass transition temperature vs. weight fraction of ED2003 in dry networks, w_{ED2003}.

Table 3
Values of some parameters determined for the dry networks

Sample	w_{ED2003}	T_g (°C)	Δc_p (J g^{-1} K^{-1})	T_c (°C)	ΔH_c (J g^{-1})	T_m (°C)	ΔH_m (J g^{-1})
EP1	0.545	−45	0.466	–	–	–	–
EP2	0.573	−40	0.548	–	–	–	–
EP3	0.600	−42	0.581	–	–	–	–
EP4	0.643	−49	0.552	−10	−1.4	12	2.1
EP5	0.701	−52	0.567	−21	−36.7	17	39.3
ED2003	1.000	−61	0.271	–	−100.5	28	107.4

Weight fraction of Br-DGEBA, w_{ED2003}; glass transition temperature, T_g; change in the specific heat, Δc_p; temperature of crystallisation, T_c; specific crystallisation enthalpy, ΔH_c; temperature of melting, T_m; and specific melting enthalpy, ΔH_m, for the dry networks and ED2003 determined from the second heating at 20 °C min^{-1}.

bulk crystal but a phase with a distribution of crystal sizes. Since our system can be considered to be a two-components one-(macro)phase system, the starting point, at room temperature, consists of water mixed with the polymer chains, that altogether constitutes the gel phase. It is then clear that the crystallization (and melting) temperature of water coming from the swollen polymer is lower than that of the pure bulk water. This effect is always present and does not depend on the size of the crystals formed. The Gibss–Thomson effect can lower even more the melting temperature but the starting point is no more that of the pure bulk water but that sorbed in the polymer network i.e. the cryoscopic effect.

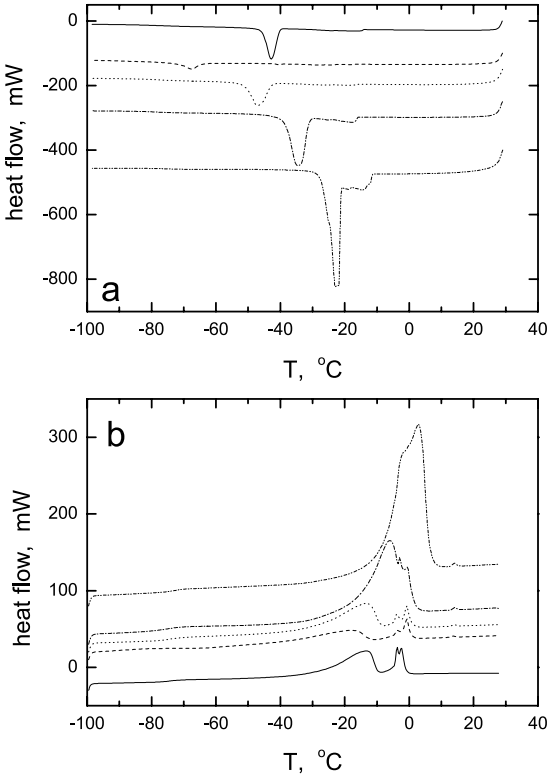

Fig. 10. DSC traces obtained for the networks swollen to equilibrium in water at 20 °C in (a) First cooling at −20 °C min^{-1} and (b) Second heating at 20 °C min^{-1}. Lines are: (—) EP1, (– – –) EP2, (…) EP3 (-·-·-·-) EP4, (-··-··-··-) EP5 and (—) ED2003.

The crystallization enthalpies allow to calculate the amount of non-crystallizable water in the swollen networks. The weight fraction of crystallizable water was calculated for each sample assuming a negligible heat of demixing of water in the polymer, and the constancy of the heat of melting of water with temperature. It was also assumed that the specific heat of melting of water in solution is not different from that of neat water. The amount of water that crystallizes or not in polymer-water systems has been explained by the phase diagram of the system. The existence of this non-crystallizable water is governed not only by specific polymer–solvent interactions [14–19], but physical phenomena taking place while the temperature of the system is lowered have also be considered [20–22]. The existence of a certain amount of a non-crystallizable solvent, in a cooling DSC scan, has been explained by high viscosity of the system as it approaches the glass transition temperature, preventing in this way the diffusion of solvent needed for continuous growth of the crystal phase. For this purpose it is useful to define the weight fraction of non-crystallizable water in swollen network, ω^* by

$$\omega^* = \frac{m^*_{water}}{m_{gel}} = 1 - \frac{1}{Q} - \frac{\Delta H_{water}}{\Delta H_{gel}} \tag{9}$$

where m_{gel} is the weight of the swollen network as determined gravimetrically, ΔH_{water} is the specific melting enthalpy of water ($\Delta H_{water} = 334$ J g^{-1}), and ΔH_{gel} is the enthalpy increment per unit weight of the swollen network as determined by the integration of the experimental DSC calorigram. Fig. 11 shows the dependence of weight fraction of non-crystallizable water in swollen network on the weight fraction of ED2003 in the dry network.

If water molecules were homogeneously distributed in the material in a single hydrophilic phase, the calculated ω^* should be the same independently of the system considered [21]. On the other hand, completely hydrophilic-hydrophobic phase-separated systems ω^* should be the higher the higher amount of hydrophilic component [23]. The evolution of ω^* shown in Fig. 11 agrees with the microphase-separated morphology of the system. It has been suggested that in network EP2, the degree of

Table 4
Values of some parameters determined for the networks swollen to equilibrium in water at 20 °C

Sample	w_{H2O}	T_g (°C)	Δc_p (J g^{-1})	T_{c1} (°C)	ΔH_{c1} (J g^{-1})	T_{c2} (°C)	ΔH_{c2} (J g^{-1})
EP1	0.548	−74	0.271	−41	−39.8	–	−8.1
EP2	0.430	−89	0.310	−65	−11.6	–	−4.9
EP3	0.490	−74	0.302	−43	−35.5	–	−4.7
EP4	0.605	−76	0.410	−30	−61.9	−17	−8.5
EP5	0.760	−73	0.311	−21	−154	−12	–

Equilibrium weight fraction of water, w_{H2O}; glass transition temperature, T_g; change in the specific heat, Δc_p; first crystallisation temperature, T_{c1}; first specific crystallisation enthalpy, ΔH_{c1}; second melting temperature, T_{c2}; second specific crystallisation enthalpy, ΔH_{c2}.

microphase separation is the highest, which is reflected also in a lower amount of non-crystallizable water compared with other networks.

4. Conclusions

A series of hydrophilic epoxy networks of various stoichiometry was prepared from α,ω-diamino terminated triblock POP/POE/POP and brominated diepoxide. The networks were studied in the dry and swollen state by dynamic mechanical analysis, small- and wide-angle X-ray scattering and differential scanning calorimetry.

In the dry state, the networks consist of Br-DGEBA chains to which POP/POE/POP copolymer chains are grafted. The networks are also microphase-separated to a degree depending on the stoichiometry but without well-defined boundaries between phases. The space scale of the network composition variation is of the nanometer order. Crystallisation and melting of POE blocks were observed by DSC and DMA during heating of the networks of lower crosslinking density ($r=1.50$ and 2.00) starting at low temperature.

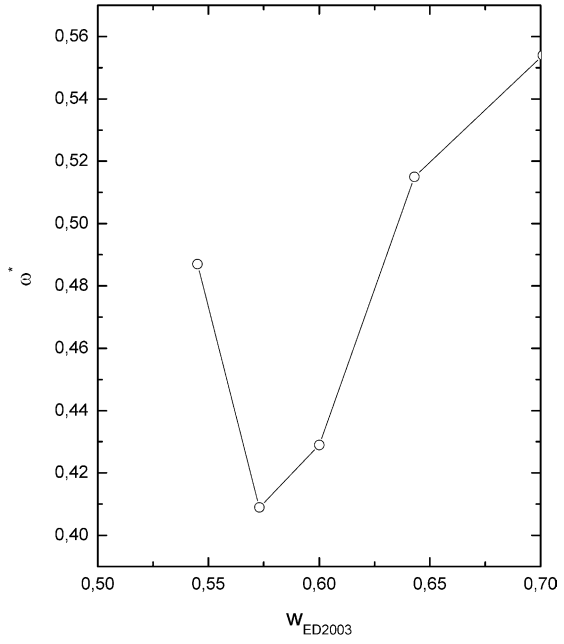

Fig. 11. Dependence of the weight fraction of non-crystallizable water in swollen network, ω^*, on the weight fraction of ED2003 in dry network.

While swelling of the networks in toluene is normal (the higher non-stoichiometry the higher swelling ratio), an anomalous swelling behaviour was found in water. This anomaly is due to the inhomogeneous swelling of the networks on the nanometer space scale depending on the degree of microphase separation in dry network. A nonstoichiometric network with the highest degree of microphase separation (EP2) and, consequently, the highest content of hydrophobic part, exhibits the lowest swelling ratio in water.

Acknowledgements

Financial support from the Ministry of Education of the Czech Republic (project MSM 11320001), Czech Science Foundation (grant No. 203/03/0600) and the Grant Agency of the Academy of Sciences of the Czech Republic (grant No. AVOZ4050913) are gratefully acknowledged.

Appendix. Calculation of network parameters

For discussion of some experimental results, structural parameters of the networks have been calculated using the theory of branching processes based on the following (rather rough) assumptions:

(a) ED2003 consists of molecules terminated by two primary amino groups; and all the four amino hydrogens have independent reactivity.
(b) Br-DGEBA consists of molecules terminated by two epoxy groups of independent reactivity.
(c) Reactivities of the hydrogens in primary and secondary amino groups are equal and independent of the extent of reaction.
(d) Formation of finite-range cyclic structures is negligible.

The notation of the reactive groups is: A = amino hydrogen, B = epoxy, as shown in Fig. 1. The key role in calculation of the network structure is played by the extinction probabilities of the oriented chemical bonds,

which link the reactive molecules. The orientation of a bond IJ (formed by reaction of groups I and J) means that this bond originates at a site of a molecule where was group I and ends at a site of another molecule where was group J. The extinction probability is defined as the probability that the bond has finite continuation only [24].

In our case there are two kinds of oriented bonds:

AB (i.e. A→B) and BA (i.e. B→A)

By the known procedure (see Refs. [3,25]), the following equations for extinction probabilities of the oriented bounds can be derived:

$$\begin{aligned} v_{AB} &= (1 - \alpha_{BA} + \alpha_{BA} v_{BA}) \\ v_{BA} &= (1 - \alpha_{AB} + \alpha_{AB} v_{AB})^3 \end{aligned} \tag{A1}$$

Conversions of amine hydrogens and epoxy groups, α_{AB} and α_{BA}, respectively, are bound by the stoichiometry:

$$r\alpha_{AB} = \alpha_{BA} \tag{A2}$$

where r is the initial molar ratio of reactants defined by

$$r = \frac{2[NH_2]_0}{[E]_0} = \frac{2n_{ED2003}}{n_{Br-DGEBA}}, \tag{A3}$$

where n_{ED2003} and $n_{Br\text{-}DGEBA}$, are molar fractions of ED2003 and Br-DGEBA in the system, respectively.

The weight fraction of sol, w_S, is given by the material with bonds of finite continuation only:

$$\begin{aligned} w_S = {} & w_{ED2003}(1 - \alpha_{AB} + \alpha_{AB} v_{AB})^4 \\ & + w_{Br-DGEBA}(1 - \alpha_{BA} + \alpha_{BA} v_{BA})^2 \end{aligned} \tag{A4}$$

where w_{ED2003} and $w_{Br\text{-}DGEBA}$ are weight fractions of the components in the system.

According to classic theories of rubber elasticity, equilibrium Young modulus of a polymer network should lie between two limits corresponding to moduli of affine and phantom network, E_{aff} and E_{ph}, respectively,

$$E_{ph} \le E \le E_{aff}$$

which are related to numbers of elastically active chains, ν_a, and cycle rank, ξ, by

$$E_{aff} = \frac{3\nu_a RT}{V^0} = 3RT\left(\frac{\nu_a}{N}\right)\left(\frac{N}{V^0}\right) \tag{A5}$$

and

$$E_{ph} = \frac{3\xi RT}{V^0} = 3RT\left(\frac{\xi}{N}\right)\left(\frac{N}{V^0}\right) \tag{A6}$$

where V^0 is volume of the network in the reference state of its formation and N is the number of molecules (ED2003 and Br-DGEBA) in mol in the initial reaction mixture.

Every elastically active network chain is terminated by two junctions with three bonds with infinite continuation (elastically active junctions) whose number per one molecule of the initial system, μ_a/N, is:

$$\begin{aligned} \frac{\mu_a}{N} = {} & 2n_{ED2003}\alpha_{AB}^4(1 - v_{AB})^4 + 4n_{ED2003}\alpha_{AB}^3(1 - v_{AB})^3 \\ & \times(1 - \alpha_{AB} + \alpha_{AB} v_{AB}) \end{aligned} \tag{A7}$$

In our case, the number of elastically active chains and cycle rank are simply:

$$\nu_a = \frac{3}{2}\mu_a \tag{A8}$$

and

$$\xi = \nu_a - \mu_a = \frac{1}{3}\nu_a = \frac{1}{2}\mu_a \tag{A9}$$

Ratio N/V^0 can be expressed using density of the network in the reference state, d^0 as

$$\frac{N}{V^0} = \frac{1}{2}d^0(w_{ED2003}c_{NH2} + w_{Br-DGEBA}c_E) \tag{A10}$$

where c_{NH2} and c_E are concentrations of amino and epoxy groups in ED2003 and Br-DGEBA, respectively.

In the case of full conversion of minor (epoxy) groups, $\alpha_{BA} = 1$, $\alpha_{AB} = 1/r$, and

Eqs. A1, A4–A6 convert to

$$v_{AB} = v_{BA} \equiv v = 1 + \frac{r}{2}(\sqrt{4r - 3} - 3) \tag{A11}$$

$$\begin{aligned} w_S &= w_{ED2003}\left(1 - \frac{1}{r} + \frac{v}{r}\right)^4 + w_{Br-DGEBA}v^2 \\ &= \frac{1}{rc_E + 2c_{NH2}}\left[rc_E\left(1 - \frac{1}{r} + \frac{v}{r}\right)^4 + 2c_{NH2}v^2\right], \end{aligned} \tag{A12}$$

$$\begin{aligned} E_{ph} = \frac{1}{3}E_{aff} = {} & \frac{3}{2}d^0RT \\ & \times \frac{rc_Ec_{NH2}}{rc_E + 2c_{NH2}}\left(\frac{1 - v}{r}\right)^3\left(2 - \frac{1 - v}{r}\right) \end{aligned} \tag{A13}$$

where r lies in the interval $1 \le r \le 3$.

References

[1] May CA, editor. Epoxy resins. Chemistry and technology. New York: Marcel Dekker; 1988.
[2] Ellis B, editor. Epoxy resins. London: Blackie; 1993.
[3] Dušek K. Adv Polym Sci 1986;78:1.
[4] Meloun J, Krakovský I, Nedbal J, Ilavský M. Eur Polym J 2000;36:2327.
[5] Beck Tan NC, Bauer BJ, Pleštil J, Barnes JD, Liu D, Matějka L, Dušek K, Wu WL. Polymer 1999;40:4603.
[6] Kratky O, Pilz J, Schmidt PJ. J Colloid Interface Sci 1966;61:24.
[7] Pleštil J, Hlavatá D. Polymer 1988;29:512.
[8] Vonk CG. J Appl Crystallogr 1973;6:81.

[9] Kratky O. Prog Biophys 1963;13:105.
[10] Grillet AC, Galy J, Pascault JP, Bardin I. Polymer 1989;30:2094.
[11] Girard-Reydet E, Riccardi CC, Sautereau H, Pascault JP. Macromolecules 1995;28:7559.
[12] Matějka L, Dušek K. Polymer 1991;32:3195.
[13] Matějka L. Macromolecules 2000;33:3611.
[14] Corkhill PH, Jolly AM, Ng CO, Tighe BJ. Polymer 1987;28:1758.
[15] Barnes A, Corkhill PH, Tighe BJ. Polymer 1988;29:2191.
[16] Hofer K, Mayer E, Johari GP. J Phys Chem 1990;94:2689.
[17] Quinn FX, Kampff E, Smyth G, McBrierty VJ. Macromolecules 1988; 21:3191.
[18] Smyth G, Quinn FX, McBrierty VJ. Macromolecules 1988;21:3198.
[19] Ishikiriyama K, Todoki M. J Polym Sci B: Polym Phys 1990;94:2689.
[20] Rault J, Gref R, Ping ZH, Nguyen QT, Néel J. Polymer 1995;36:1655.
[21] Rault J, Lucas A, Neffati R, Monleón Pradas M. Macromolecules 1997;30:7866.
[22] Franks F. In: Hemminger W, editor. Thermal analysis, vol. 2.
[23] Salmerón Sánchez M, Gallego Ferrer G, Monleón Pradas M, Gómez Ribelles JL. Macromolecules 2003;36:860.
[24] Dobson GR, Gordon M. J Chem Phys 1965;43:705.
[25] Krakovský I, Havránek A, Ilavský M, Dušek K. Colloid Polym Sci 1988;266:324.